Rational Constitutive Formulation for Earthquake Ruptures and Physical Scaling of Their Scale-Dependence

Mitiyasu Ohnaka
The University of Tokyo, and University College London

- Ohnaka, M., Earthquake cycles and physical modeling of the process leading up to a large earthquake, *Earth Planets Space*, **56**, 773-793, 2004.
- Ohnaka, M., Perspectives: Rupture in the Laboratory, *Science,* **303**(5665), 1788-1789, 2004 (19 March 2004 Issue).
- Ohnaka, M., A constitutive scaling law and a unified comprehension for frictional slip failure, shear fracture of intact rock, and earthquake rupture, *J. Geophys. Res.*, **108**(B2), 2080, doi:10.1029/2000JB000123, 2003.
- Ohnaka, M., A physical scaling relation between the size of an earthquake and its nucleation zone size, *Pure Appl. Geophys.*, **157**, 2259-2282, 2000.
- Ohnaka, M., and L.-f. Shen, Scaling of the shear rupture process from nucleation to dynamic propagation: Implications of geometric irregularity of the rupturing surfaces, *J. Geophys. Res.*, **104**, 817-844, 1999.

Prerequisites for Constitutive Formulation for Earthquake Ruptures

- The seismogenic layer and individual faults therein are inherently in-homogeneous.
- Earthquake ruptures are scale-dependent; that is, some of the physical quantities inherent in the rupture exhibit scale-dependence.

Fault Inhomogeneity

- Seismological Evidence

  Earthquake faults comprise strong portions called "asperities" or "barriers", with the rest of the fault having low (or little) resistance to rupture growth.

- Geological Evidence

  A real fault consists of a number of discrete segments, and individual segments are non-planar and exhibit geometric irregularity that contains various wavelength components.

The sites of the zones of segment stopover and/or interlocking asperities are strong, and possibly have the strength equal to (or close to) that of intact rock.

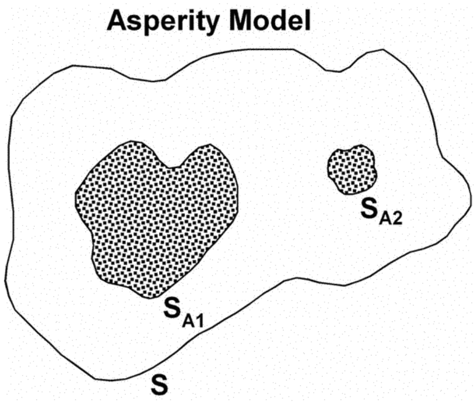

$$G_c = \int_0^{D_c} [\tau(D) - \tau_r] dD$$ (Palmer and Rice, 1973)

$$= \frac{1}{2} \Gamma \Delta\tau_b D_c$$ (Ohnaka and Yamashita, 1989)

where

$$\Gamma = \int_0^1 \frac{\sigma(Y)}{\sqrt{Y}} dY$$

- Earthquake ruptures occur on pre-existing faults, with gouge particles in the intervening fault surfaces.
- Earthquake faults are inhomogeneous, and individual faults comprise strong local areas of high resistance to rupture growth, with the rest of the fault having low (or little) resistance to rupture growth.
- The size/magnitude of an earthquake is prescribed by the driving force, which is the elastic strain energy stored in the elastic medium surrounding the fault by sustaining fault strength at such strong local areas.

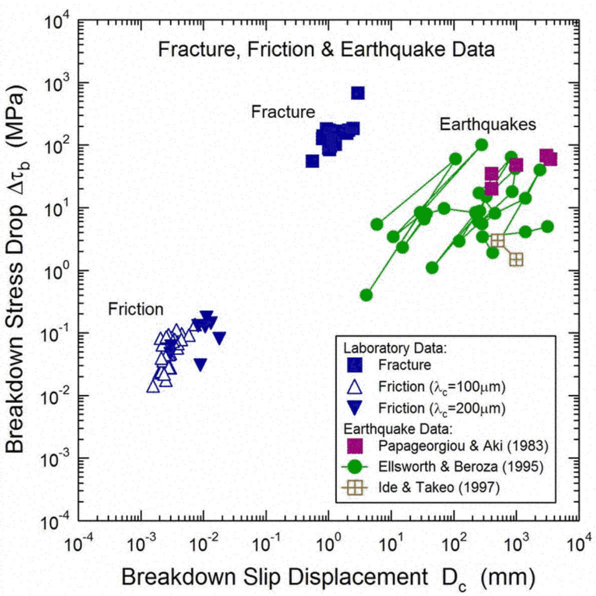

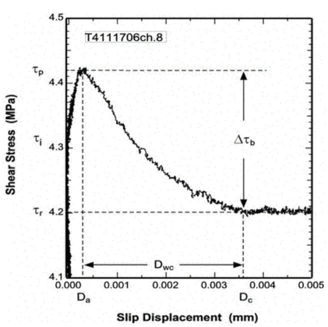

Scale-Dependence of Physical Quantities Inherent in the Rupture

- **Apparent Shear Rupture Energy**

$$G_c = \int_0^{D_c} [\tau(D) - \tau_r] dD = \frac{\Gamma}{2} \Delta\tau_b D_c$$

- **Slip Acceleration**

$$\ddot{D}_{max} = \frac{\Gamma^2 \phi''_{max}}{\pi^4} \left(\frac{V}{C(V)} \frac{\Delta\tau_b}{\mu} \right)^2 \frac{1}{D_c}$$

- **Nucleation Zone Length**

$$L_c = \frac{1}{k} \frac{\mu}{\Delta\tau_b} D_c$$

$$M_0 = c_1 c_2 \left(\frac{k\kappa\Gamma}{4} \right)^3 \left(\frac{S_{A1}}{aS} \right)^3 \left(\frac{\Delta\tau_b^{A1}}{\overline{\Delta\tau}} \right)^6 \mu (2L_c)^3$$

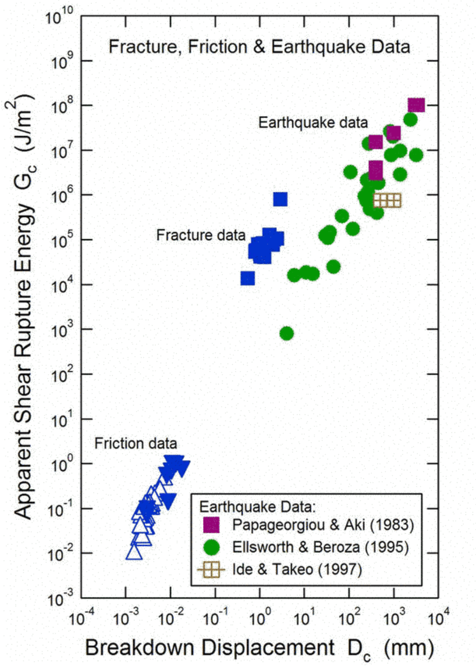

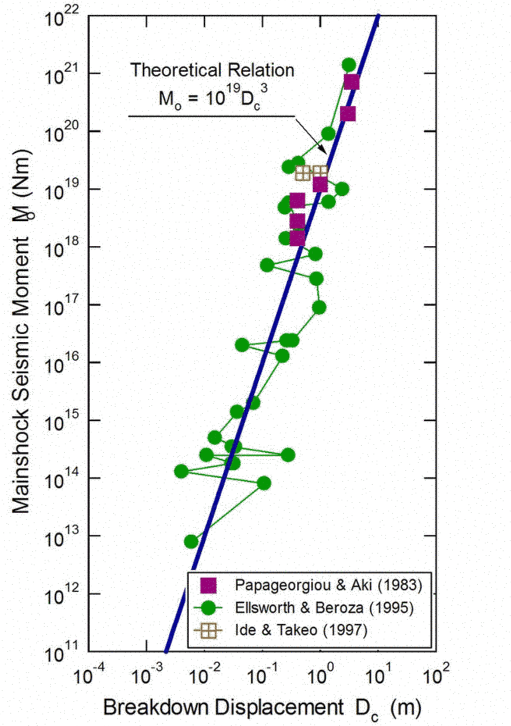

$$M_o = c_1 c_2 (\kappa\Gamma/2)^3 (S_{A1}/aS)^3 (\mu/\Delta\tau)^3 (\Delta\tau_b/\Delta\tau)^3 \mu D_c^3$$

Scale-Dependence of Slip Acceleration

Peak Slip Velocity :

$$\dot{D}_{max} = \frac{\Gamma V}{\pi^2 C(V)} \frac{\Delta\tau_b}{\mu} \phi'_{max} \qquad (1)$$

Peak Slip Acceleration :

$$\ddot{D}_{max} = \frac{\Gamma^2 \phi''_{max}}{\pi^2} \left(\frac{V}{C(V)} \frac{\Delta\tau_b}{\mu} \right)^2 \frac{1}{D_c} \qquad (2)$$

From (1) and (2), we have

$$\ddot{D}_{max} = \frac{h}{D_c} \dot{D}^2_{max} \qquad (3)$$

where

$$h = \phi''_{max} / (\phi'_{max})^2 \qquad (4)$$

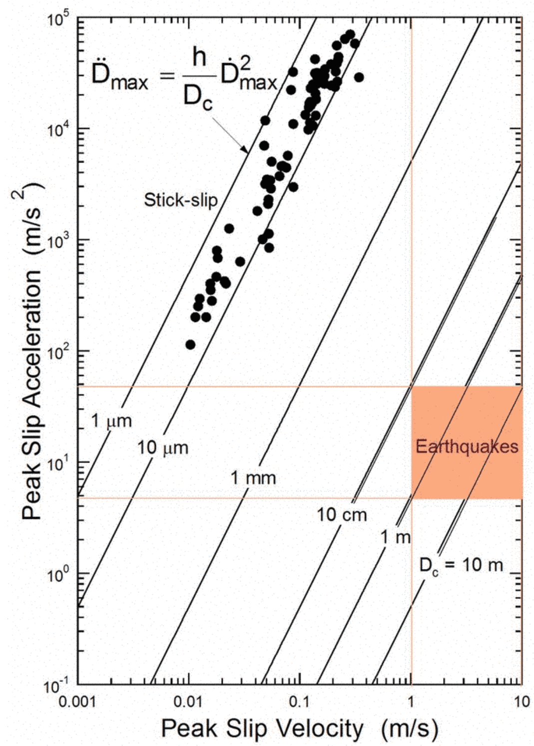

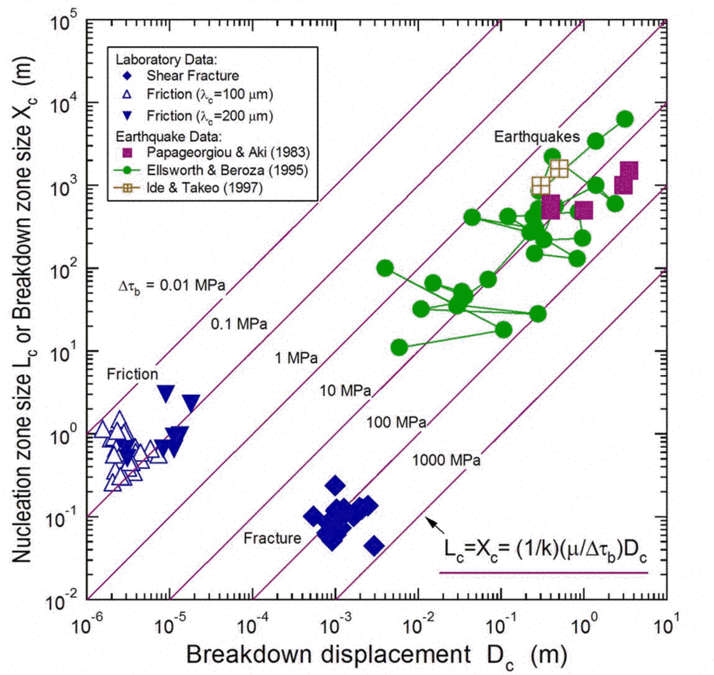

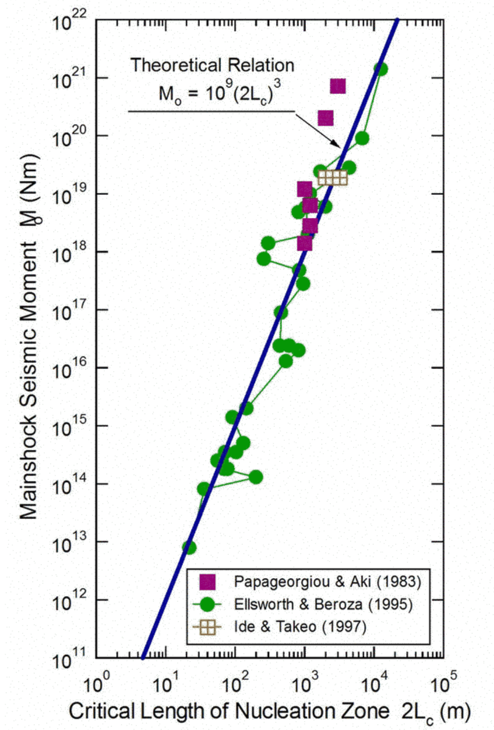

$$M_o = c_1 c_2 (k\kappa\Gamma/4)^3 (S_{A1}/aS)^3 (\Delta\tau_b/\Delta\tau)^6 \mu (2L_c)^3$$

Rational Constitutive Formulation for Earthquake Ruptures

- The constitutive law for earthquake ruptures must be a unifying law that governs both frictional slip failure and the shear fracture of intact rock.
- The constitutive law for earthquake ruptures must also be formulated so as to incorporate the scaling property.

Rational Constitutive Formulation for Earthquake Ruptures

- To unify frictional slip failure and the shear fracture of intact rock, the constitutive law must be formulated as a slip-dependent law.
- To account for scale-dependent physical quantities inherent in the rupture over a broad scale range in quantitative terms, the constitutive law should also be formulated as a slip-dependent law.

Why It Should be Formulated as a Slip-Dependent Law for Physical Scaling of the Scale-Dependent Quantities?

- D_c, defined as the breakdown slip in the framework of slip-dependent formulation, straightforwardly represents the slip displacement at the end of the breakdown process, which is a specific length scale inherent in the breakdown process.
- Therefore, D_c is most appropriate as a scaling parameter that plays a fundamental role in scaling the scale-dependent physical quantities.

Scale-Dependence of D_c

D_c scales with the characteristic length λ_c according to the following law:

$$D_c = (1/\beta)^{1/M}(\Delta\tau_b/\tau_p)^{1/M}\lambda_c$$

Physical Grounds:

- The shear rupture that proceeds on an irregular interface is governed by not only nonlinear physics of the constitutive law but also geometric properties of the rupture surface irregularity.
- The fundamental cause of the scaling property lies at λ_c defined as the predominant wavelength that represents geometric irregularity of the rupturing surfaces.

Slip-Dependent Constitutive Relation

$$\tau = f(D; \dot{D}, \lambda_c, \sigma_n^{eff}, T, CE)$$

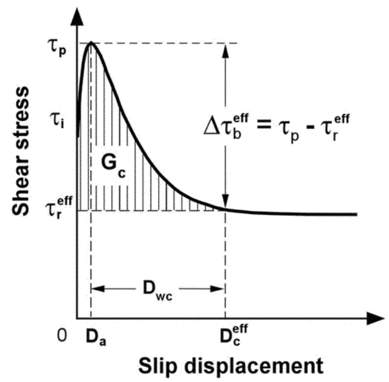

$$(\tau_i, \tau_p, \tau_r, D_a, D_c) \rightarrow (\tau_i, \tau_p, \Delta\tau_b, D_a, D_c)$$

$$G_c = \int_0^{D_c} [\tau(D) - \tau_r] dD$$

$$\tau_p = f(\sigma_n^{eff})[1 + \alpha \ln(\dot{D}/\dot{D}_0)]$$

$$D_c = a(\Delta\tau_b/\tau_p)^m \lambda_c \quad \text{and} \quad D_a = (1 - c_1)D_c$$

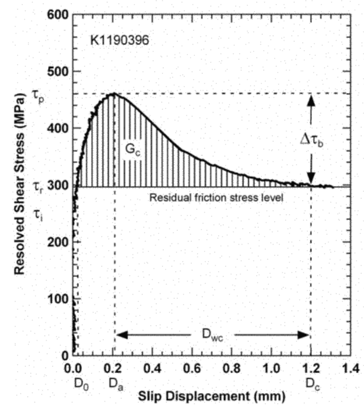

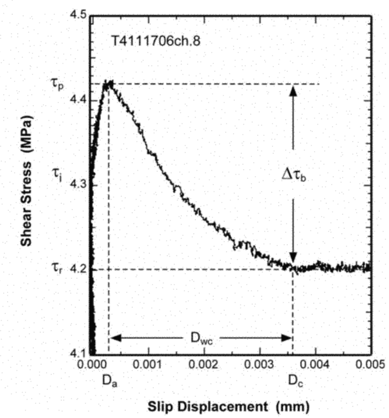

Unification Under Slip-Dependent Constitutive Formulation

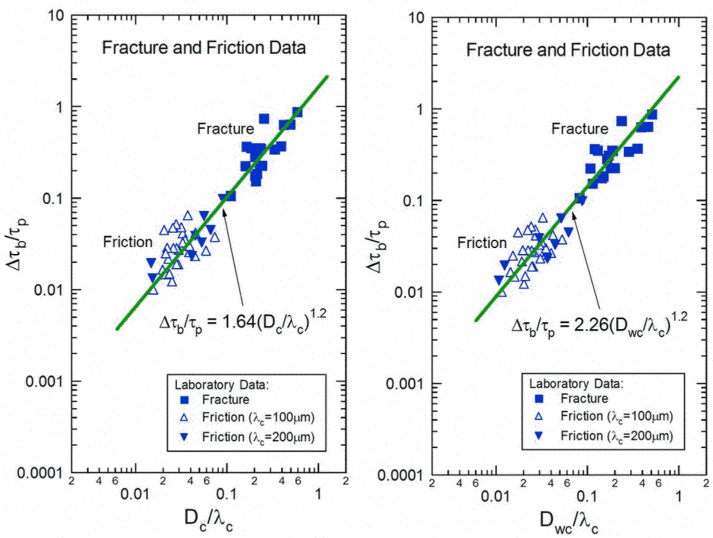

$D_{wc} = (1.64/2.26)^{1/1.2} D_c = 0.766 D_c$

$D_a = D_c - D_{wc} = 0.234 D_c$

Unification Under Slip-Dependent Constitutive Formulation

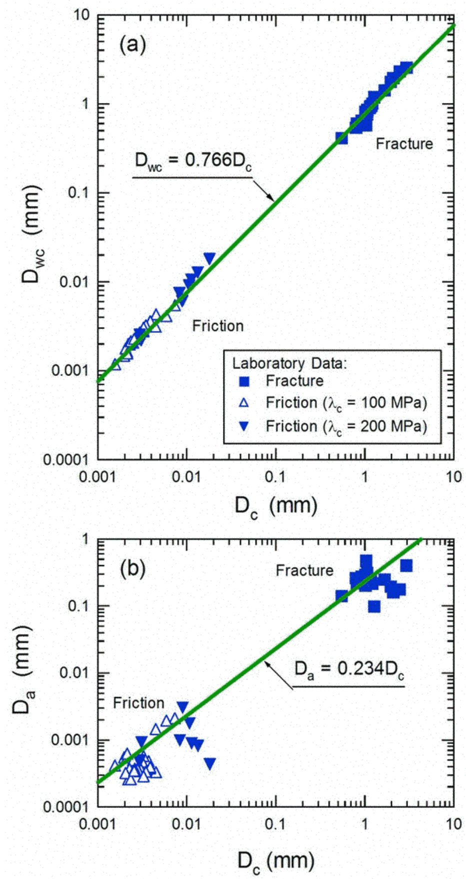

Unification Under Slip-Dependent Constitutive Formulation

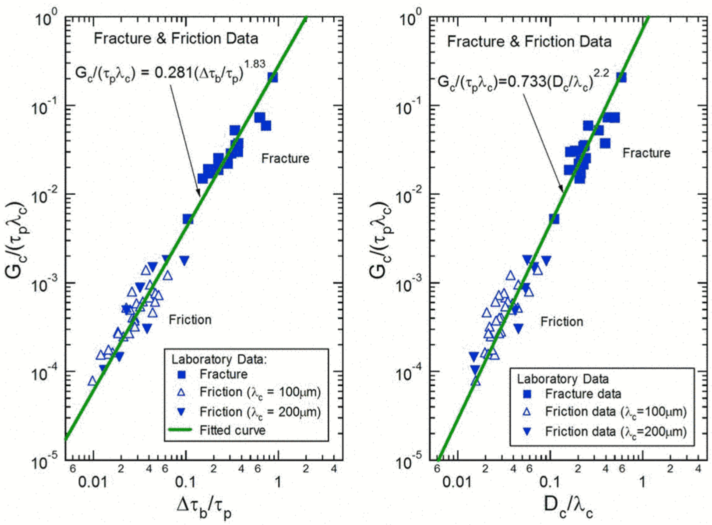

$$G_c = \int_0^{D_c} \{\tau(D) - \tau_r\}\, dD = \frac{\Gamma}{2}\Delta\tau_b D_c = \frac{\Gamma}{2}\left(\frac{1}{\beta}\right)^{1/M}\Delta\tau_b\left(\frac{\Delta\tau_b}{\tau_p}\right)^{1/M}\lambda_c$$

$$\frac{G_c}{\tau_p\lambda_c} = \frac{\Gamma}{2}\left(\frac{1}{\beta}\right)^{\frac{1}{M}}\left(\frac{\Delta\tau_b}{\tau_b}\right)^{\frac{M+1}{M}} = \frac{\Gamma\beta}{2}\left(\frac{D_c}{\lambda_c}\right)^{M+1}$$

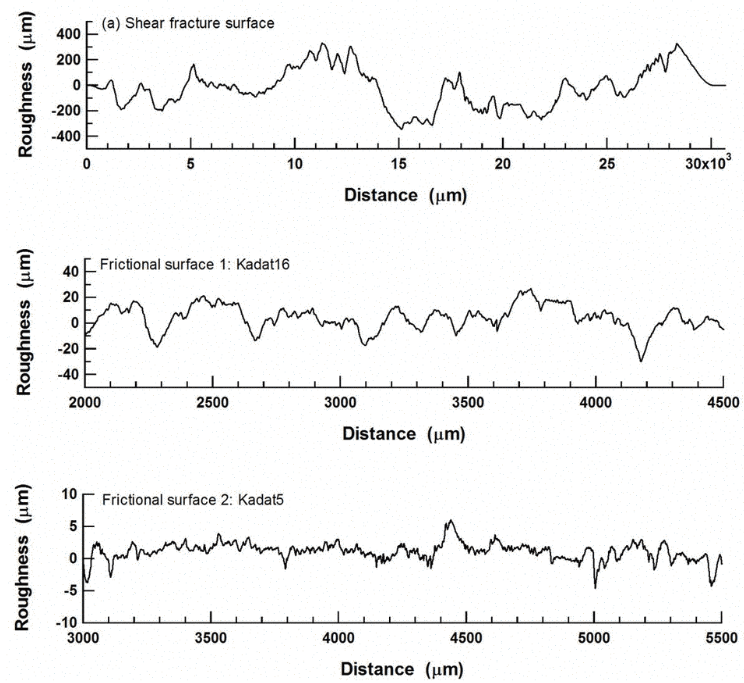

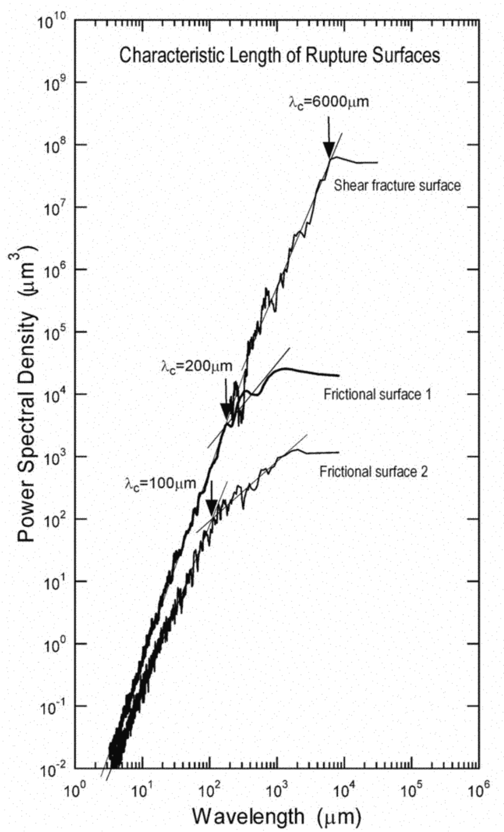

Unification Under Slip-Dependent Constitutive Formulation

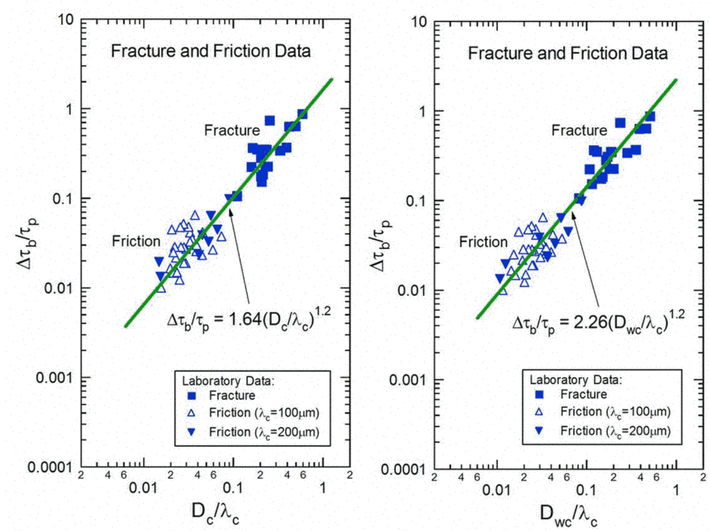

$$D_{wc} = (1.64/2.26)^{1/1.2} D_c = 0.766 D_c$$

$$D_a = D_c - D_{wc} = 0.234 D_c$$

$$\boldsymbol{D_c = (1/\beta)^{1/M} (\Delta\tau_b/\tau_p)^{1/M} \lambda_c = 0.662 (\Delta\tau_b/\tau_p)^{0.833} \lambda_c}$$

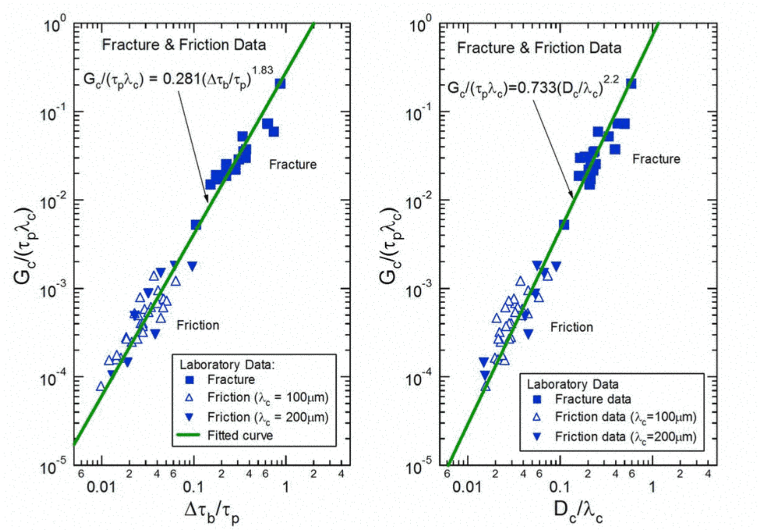

Fracture & Friction Data
$G_c/(\tau_p\lambda_c) = 0.281(\Delta\tau_b/\tau_p)^{1.83}$
Fracture
Friction
Laboratory Data:
Fracture
Friction (λ_c = 100μm)
Friction (λ_c = 200μm)
Fitted curve
$G_c/(\tau_p\lambda_c)$
$\Delta\tau_b/\tau_p$
Fracture & Friction Data
$G_c/(\tau_p\lambda_c)=0.733(D_c/\lambda_c)^{2.2}$
Fracture
Friction
Laboratory Data
Fracture data
Friction data (λ_c=100μm)
Friction data (λ_c=200μm)
D_c/λ_c

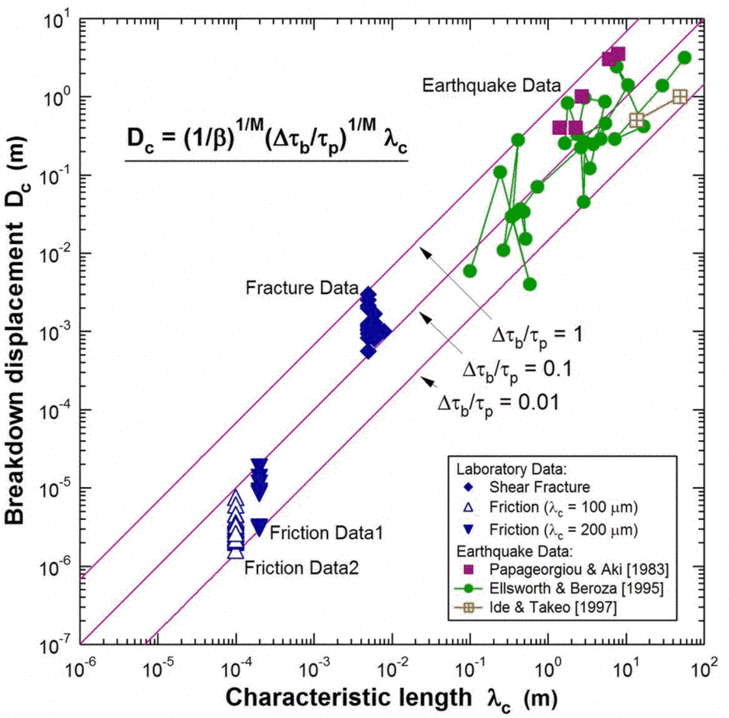

$D_c = (1/\beta)^{1/M}(\Delta\tau_b/\tau_p)^{1/M}\,\lambda_c$
Earthquake Data
Fracture Data
Friction Data1
Friction Data2
$\Delta\tau_b/\tau_p = 1$
$\Delta\tau_b/\tau_p = 0.1$
$\Delta\tau_b/\tau_p = 0.01$
Laboratory Data:
Shear Fracture
Friction (λ_c = 100 μm)
Friction (λ_c = 200 μm)
Earthquake Data:
Papageorgiou & Aki [1983]
Ellsworth & Beroza [1995]
Ide & Takeo [1997]
Breakdown displacement D_c (m)
Characteristic length λ_c (m)

Both D_c and λ_c are larger for a larger earthquake fault. Why?

1. Rupture surfaces of an inhomogeneous fault cannot be flat planes but they necessarily exhibit geometric irregularity.
2. A large fault includes geometrically large, local areas of high resistance to rupture growth (in a statistical sense).
3. The irregular rupture surfaces of such geometrically large local areas contain a long predominant wavelength component λ_c in themselves.
4. A large amount of D_c is necessarily required for breaking down such a geometrically large local area containing large λ_c.

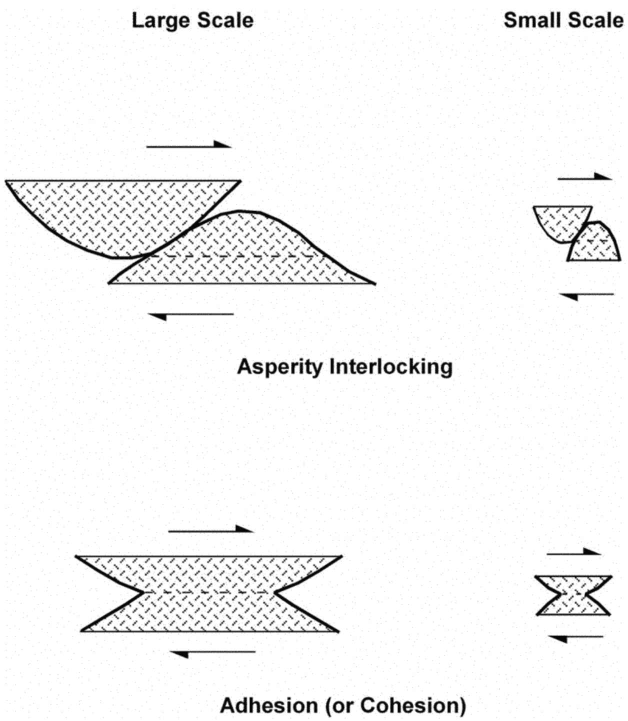

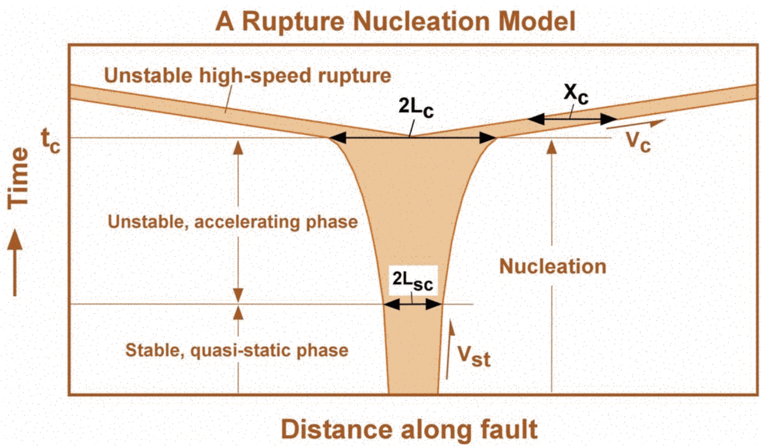
A Rupture Nucleation Model
Unstable high-speed rupture
2Lc
Xc
Vc
tc
Time
Unstable, accelerating phase
2Lsc
Nucleation
Stable, quasi-static phase
Vst
Distance along fault

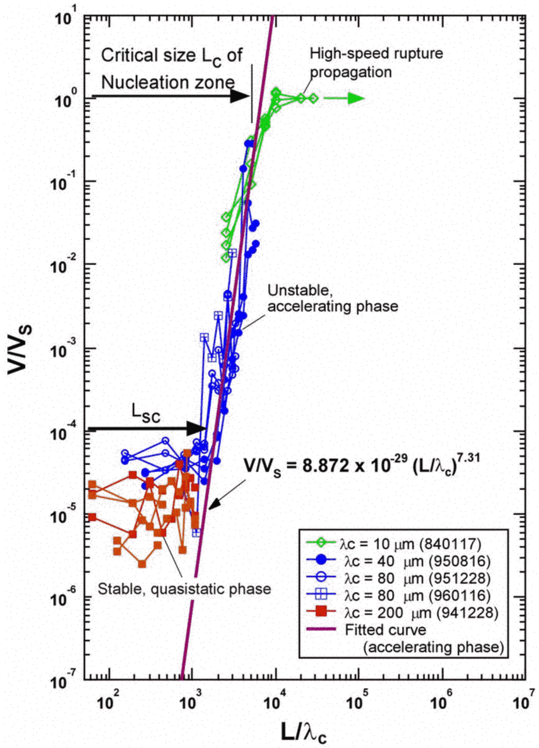
Critical size Lc of Nucleation zone
High-speed rupture propagation
Unstable, accelerating phase
Lsc
V/Vs = 8.872 x 10^-29 (L/λc)^7.31
Stable, quasistatic phase
λc = 10 μm (840117)
λc = 40 μm (950816)
λc = 80 μm (951228)
λc = 80 μm (960116)
λc = 200 μm (941228)
Fitted curve (accelerating phase)
V/Vs
L/λc

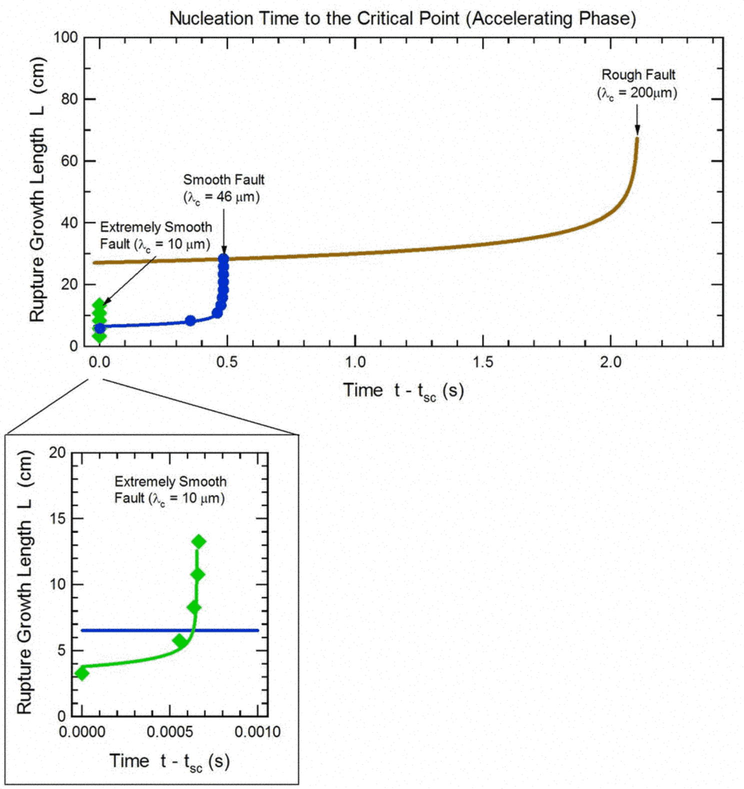
Nucleation Time to the Critical Point (Accelerating Phase)
Rupture Growth Length L (cm)
Time t - t_sc (s)
Rough Fault (λc = 200μm)
Smooth Fault (λc = 46 μm)
Extremely Smooth Fault (λc = 10 μm)
100
80
60
40
20
0
0.0
0.5
1.0
1.5
2.0
Extremely Smooth Fault (λc = 10 μm)
Rupture Growth Length L (cm)
Time t - t_sc (s)
20
15
10
5
0
0.0000
0.0005
0.0010

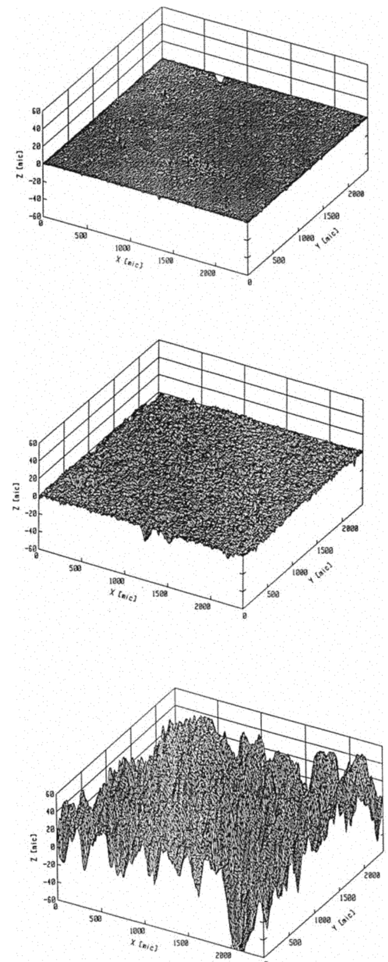

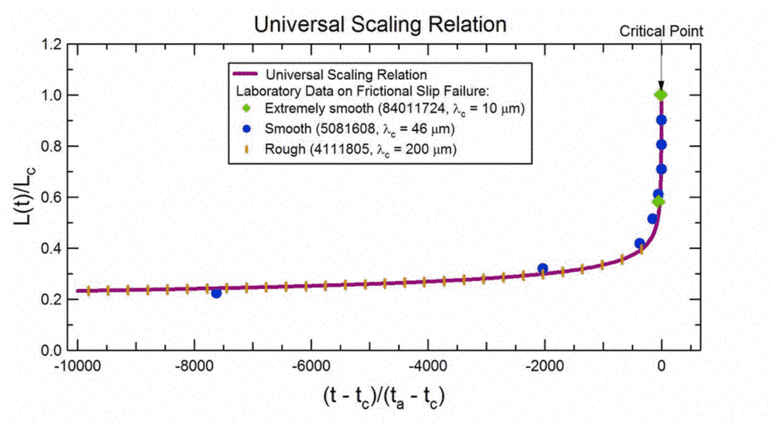

$$\frac{L(t)}{L_c} = \left(\frac{1}{1-(t-t_c)/(t_a-t_c)}\right)^{1/(n-1)}$$

where

$$\frac{t-t_c}{t_a-t_c} = \alpha(n-1)\left(\frac{L_c}{\lambda_c}\right)^{n-1}\frac{t-t_c}{(\lambda_c/V_s)}$$

Constitutive Formulation for Earthquake Ruptures

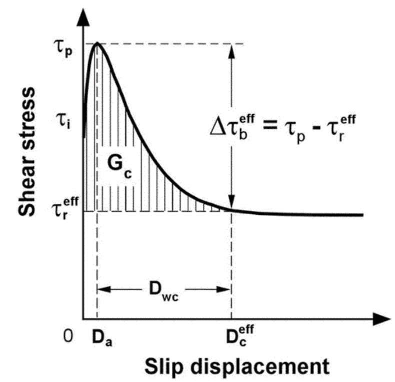

$$(\tau_i, \tau_p, \tau_r, D_a, D_c) \rightarrow (\tau_i, \tau_p, \Delta\tau_b, D_a, D_c)$$

$$\tau(D,r) = \tau_p(r) - \Delta\tau_b(r)\left[1 - h(D,r)\exp\left(-H(r)\left(\frac{D}{D_a(r)} - 1\right)\right)\right]$$

where $h(D_a, r) = 1$ and

$$h(D,r)\exp\left[-H(r)\left(\frac{D}{D_a(r)} - 1\right)\right] \rightarrow 0 \quad \text{for sufficiently large } D$$

Constitutive Formulation for Earthquake Ruptures

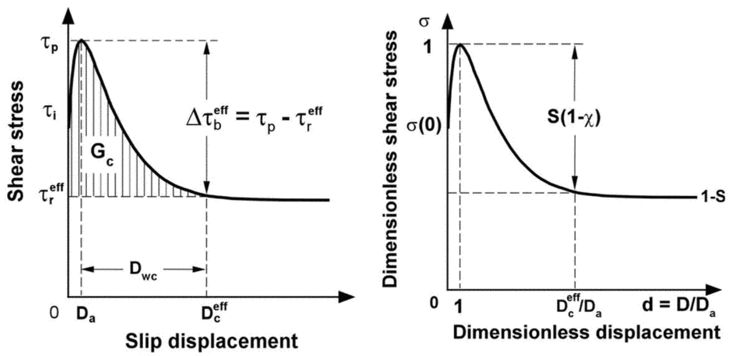

$$\sigma(d,r) = 1 - S(r)\{1 - [1 + A(r)\log(1 + B(r)(d-1))]\exp[-A(r)B(r)(d-1)]\}$$

where $\sigma(d,r) = \tau(d,r)/\tau_p(r)$, and $d = D/D_a(r)$.

$$(\tau_p, \tau_i, \Delta\tau_b^{eff}, D_a, D_c^{eff}) \rightarrow (\tau_p, D_a, S, A, B)$$

$$S(r) = \frac{\Delta\tau_b^{eff}(r)/(1-\chi)}{\tau_p(r)}$$

$$1 - [1 + A(r)\log(1 - B(r))]\exp[A(r)B(r)] = \frac{\tau_p(r) - \tau_i(r)}{\Delta\tau_b^{eff}(r)/(1-\chi)}$$

$$\left[1 + A(r)\log\left(1 + B(r)\left(\frac{D_c^{eff}(r)}{D_a(r)} - 1\right)\right)\right]\exp\left(-A(r)B(r)\left(\frac{D_c^{eff}(r)}{D_a(r)} - 1\right)\right) = \chi$$

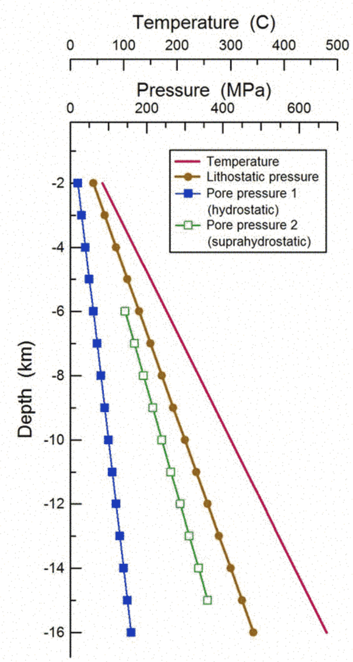

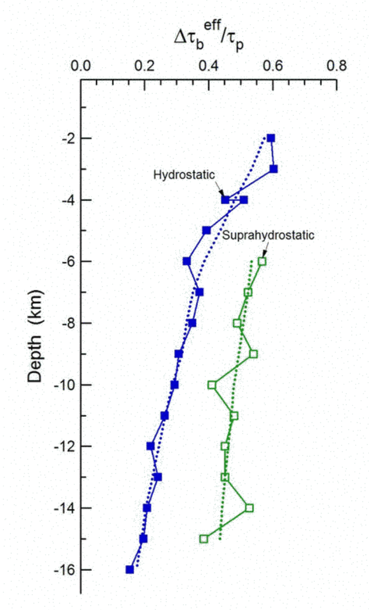

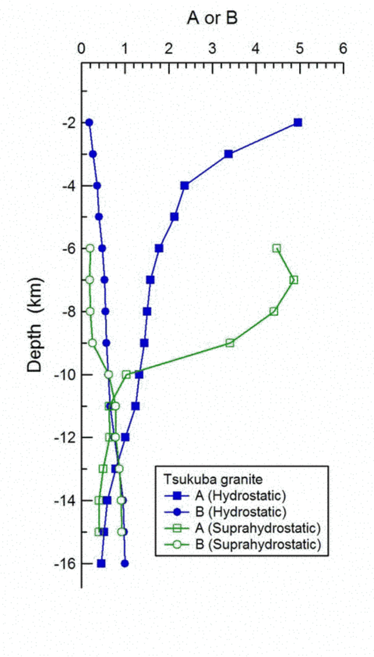

$$S = \frac{\Delta\tau_b^{eff}}{\tau_p}\frac{1}{1-\chi}$$

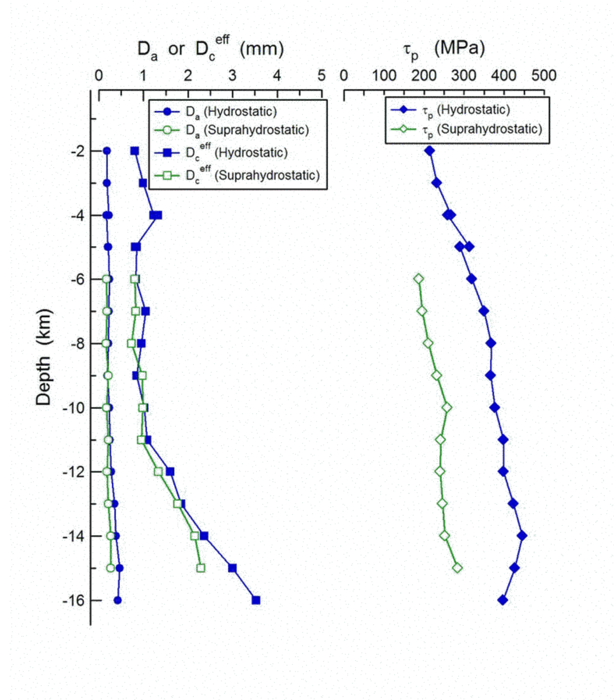

- Whether a nucleated shear rupture rapidly reaches to the phase of dynamic, steady propagation at a high speed close to the shear wave velocity or it slowly grows and takes time to reach the phase of dynamic, high speed propagation, completely depends on geometric irregularity of the rupturing surfaces.
- Let me show how the geometric irregularity greatly influences the development of shear rupture nucleation to dynamic, high speed propagation in the following several slides (for more details, see Ohnaka and Shen, J. Geophys. Res., 104, 817-844, 1999).

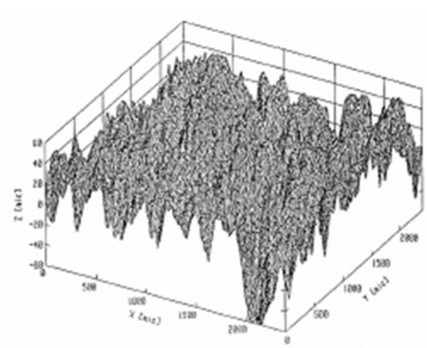

Rough fault surface

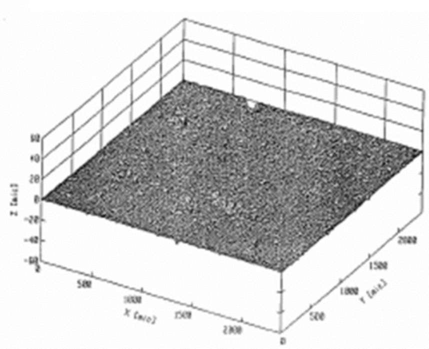

Extremely smooth fault surface

Figure 1. (continued)

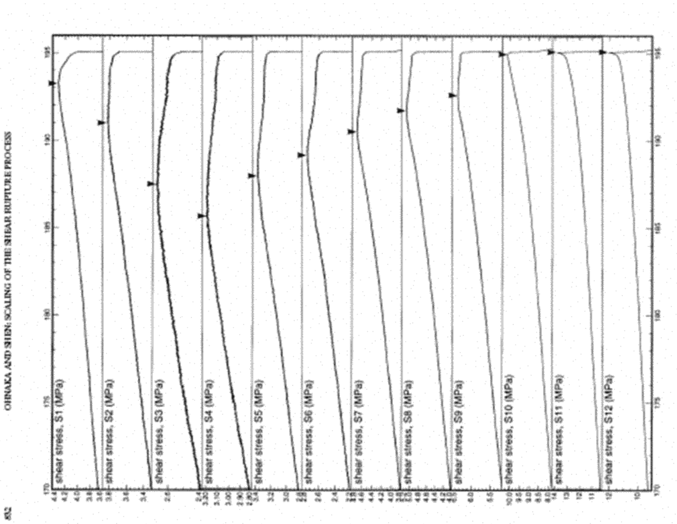

Figure 20a. An example (event T4111805) of local shear stress versus time records at 12 positions along the fault for a slip failure event on the rough fault. Arrows denote the time when slip failure began to occur locally.

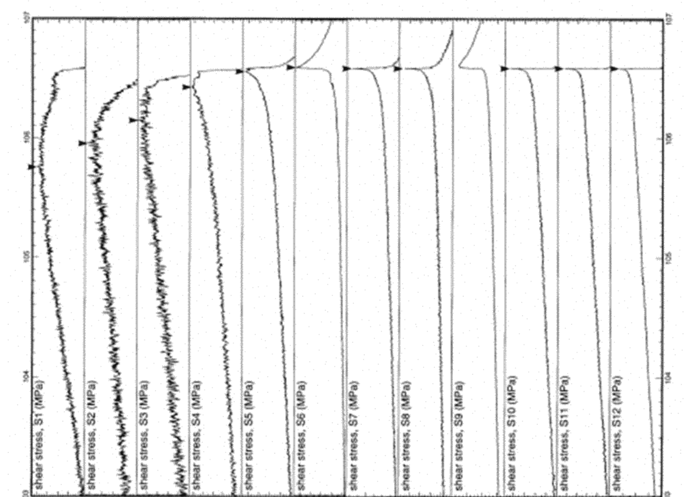

Figure 23a. An example (event T5061608) of local shear stress versus time records at 12 positions along the fault for a slip failure event on the smooth fault. Arrows denote the time when slip failure began to occur locally.

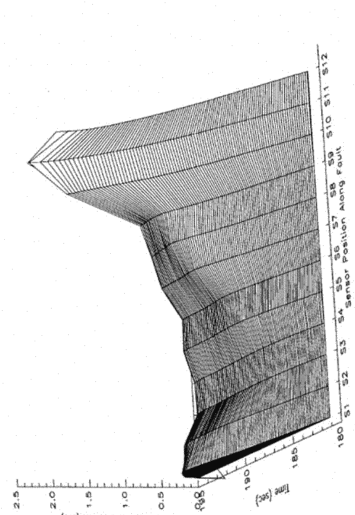

Figure 8. Time and spatial variations of differential shear stresses (τ_{d180}) recorded locally at 12 positions along the fault during the nucleation for the failure event shown in Figures 5–7 (rough fault).

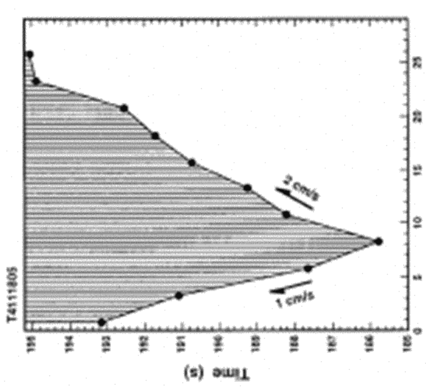

Figure 21. Space-time view of the nucleation zone on the rough fault for the event (T4111805) shown in Figure 20. The hatched portion indicates the zone in which the slip weakening is proceeding with time (see Figure 9).

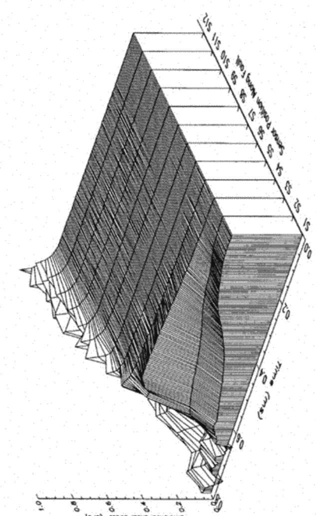

Figure 18. Time and spatial variations of differential shear stresses (τ_{d0}) recorded locally at 12 positions along the fault during the nucleation for a slip failure event on the extremely smooth fault.

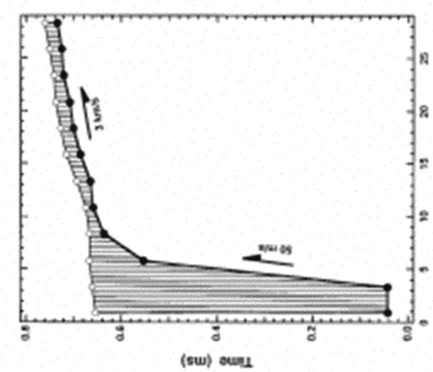

Figure 26. Space-time view of the nucleation zone for a slip failure event (E4011?comb) on the extremely smooth fault. The hatched portion indicates the zone in which the slip weakening is proceeding with time.

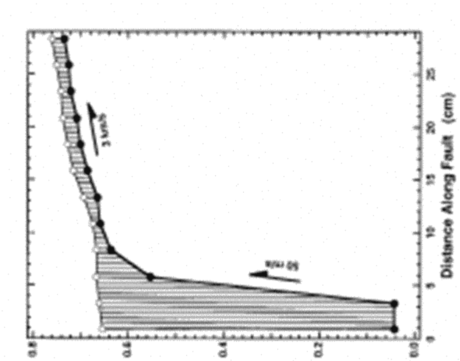

Figure 26. Space-time view of the nucleation zone for a slip failure event (E40117comb) on the extremely smooth fault. The hatched portion indicates the zone in which the slip weakening is proceeding with time.

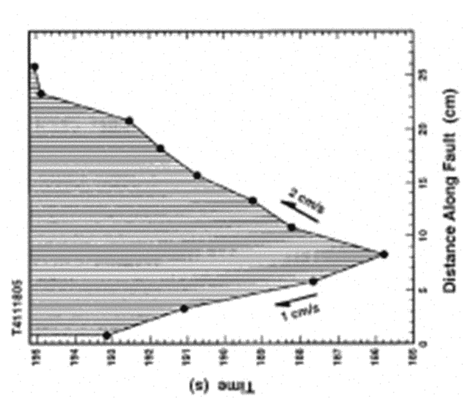

Figure 21. Space-time view of the nucleation zone on the rough fault for the event (T4111805) shown in Figure 20. The hatched portion indicates the zone in which the slip weakening is proceeding with time (see Figure 9).

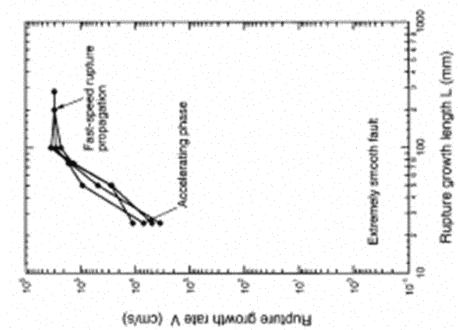

Figure 27. Plots of the logarithm of the rupture growth rate V against the logarithm of the rupture growth length L during the nucleation for events on the extremely smooth fault.

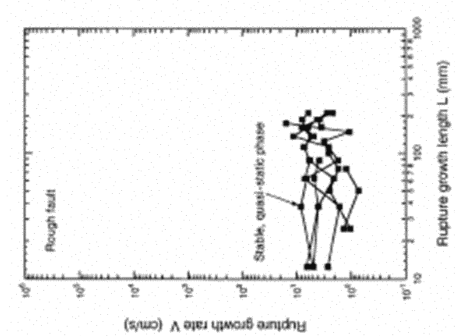

Figure 22. Plots of the logarithm of the rupture growth rate V against the logarithm of the rupture growth length L during the nucleation for events on the rough fault.

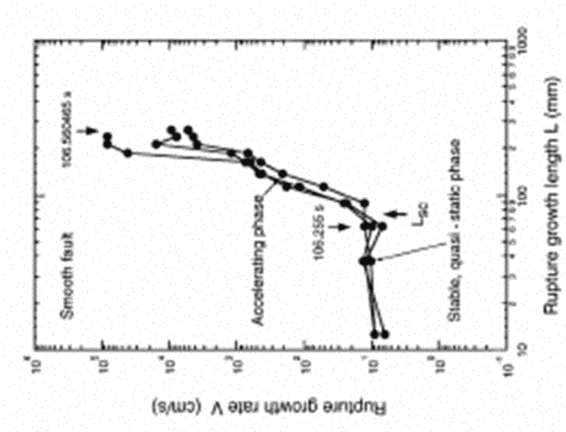

Figure 25. Plots of the logarithm of the rupture growth rate V against the logarithm of the rupture growth length L during the nucleation for events on the smooth fault. L_{sc} denotes the critical length beyond which the rupture grows at accelerating speeds, and the times t_1 = 106.255 s and t_2 = 106.560465 s are included to facilitate comparison with Figures 23 and 24.

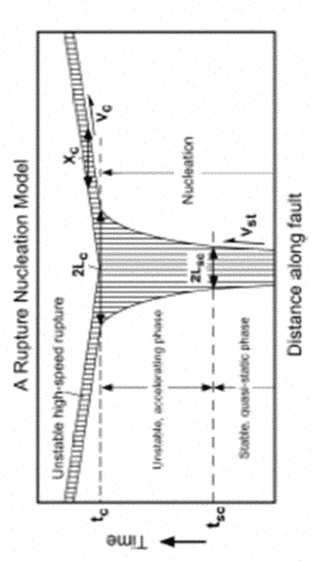

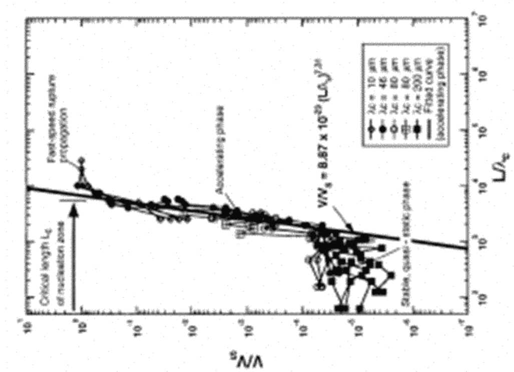

Figure 28. Log-log plots of the rupture growth rate V normalized to the shear wave velocity V_s against the rupture growth length L normalized to λ_c during the nucleation for events on the faults with different surface roughnesses.

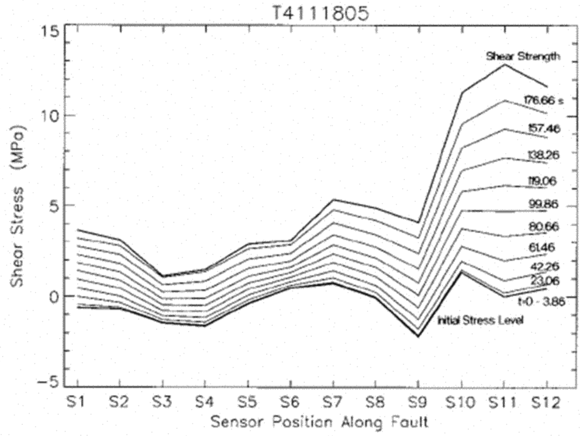

Figure 7. Nonuniform distributions of the fault strength (top thick line), initial shear stress level (bottom thick line) induced by application of the normal load (6.2 MPa), and variations of levels of local shear stresses along the fault with time for the slip failure event shown in Figures 5 and 6 (rough fault) for event T4111805. Local shear stress levels are plotted at 19.2-s intervals from $t = 3.86$ s after shear load application. Positive or negative shear stress indicates clockwise or anticlockwise shear, respectively.

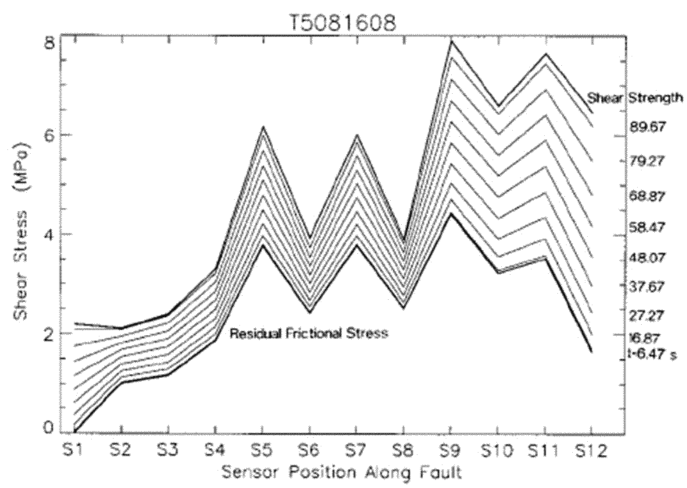

Figure 14. Nonuniform distributions of the fault strength, the residual friction stress, and variation of levels of local shear stresses along the fault with time for the slip failure event (T5081608) shown in Figures 12 and 13 (smooth fault). Local shear stress levels are plotted at 10.4-s intervals from $t = 6.47$ s after the onset of shear load application for this event.

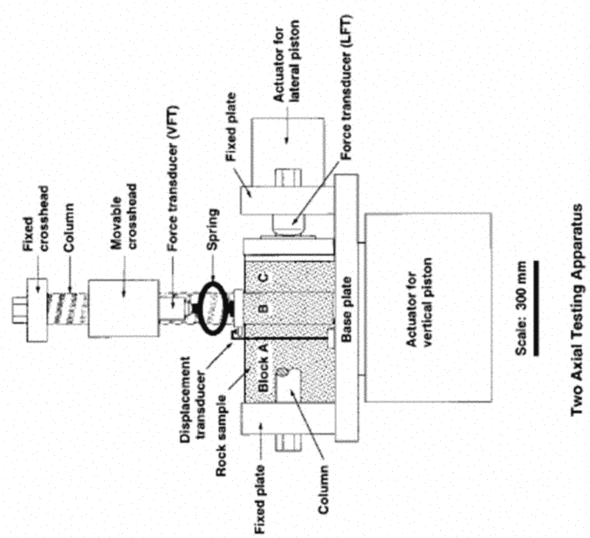

Figure 3. The configuration for the present experiments.

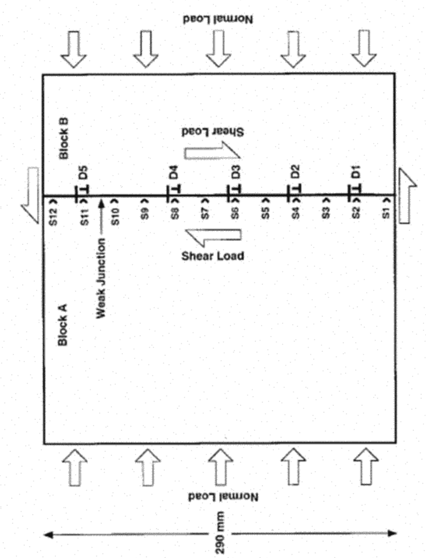

Figure 4a. Sample configuration with two types of sensors in position. S1 to S12 denote the positions at which 12 pairs of strain gauges were mounted to measure local shear strains in the direction parallel to the fault, and D1 to D5 denote the positions at which displacement sensors were mounted to measure local slips on the fault.